Asian Journal of Chemistry; Vol. 38, No. 4 (2026), 971-978
ASIAN JOURNAL OF CHEMISTRY
https://doi.org/10.14233/ajchem.2026.34988

Synthesis and Characterisation of β-Cyclodextrin-Conjugated Carboxymethyl Chitosan Derivative for Antimicrobial and Wound Healing Applications

S. RENUKADEVI[1], B. DEEPAN KUMAR[2], G. HARI HARA PRIYA[3], T. TAMIZHARUVI[1] and V. JAISANKAR[1,*]

[1]PG and Research Department of Chemistry, Presidency College (Autonomous), Chennai-600005, India
[2]Department of Chemistry, Institute of Chemical Technology, Tharamani, Chennai-600113, India
[3]PG Department of Chemistry, Shrimathi Devkunvar Nanalal Bhatt Vaishnav College for Women, Chennai-600044, India

*Corresponding author: E-mail: vjaisankar@gmail.com

Received: 1 October 2025 *Accepted*: 17 February 2026 *Published online*: 8 April 2026 AJC-22318

Chitosan can be chemically modified to form a range of derivatives to perform enhanced biological activities with enhanced solubility in water and functional properties. These alterations have tunned their applications towards biomedical fields. This work aims to synthesize the carboxymethyl derivative of chitosan selectively functionalised at the C6 carbon atom through careful masking of the C2 location. In this regard, the C2-amino group was shielded to avoid interfering with the carboxymethylation process at the C6 hydroxyl group. The functional characteristics of the chitosan derivative were further improved by conjugating it with β-cyclodextrin to form a β-cyclodextrin-carboxymethyl chitosan (CD-CMCh) derivative. Further biological potential was tested on the derivative emphasizing its significant activity against the bacteria *S. aureus* (13 ± 2 mm), *E. coli* (9 ± 1 mm) and *K. pnemoniae* (11 ± 2 mm) at the concentration of 1000 µg/mL, along with the potent activity against fungal *A. niger* (19 ± 5.7 mm, 16.37 ± 7.6 mm) and *T. viride* (13.3 ± 3.5 mm, 12.7 ± 5 mm) at the concentration 1000 and 500 µg/mL, respectively than *C. albicans*. Furthermore, the *in vitro* wound healing assay revealed a 65% wound closure, indicating substantial cell migration and regenerative potential. Results revealed that this selectively modified derivative is a flexible molecule in the production of biomedical materials and thus holds great promise for application in antimicrobial treatments and wound healing therapy.

Keywords: Biopolymer, Carboxymethyl chitosan, β-Cyclodextrin, Antimicrobial activity, Wound healing applications.

INTRODUCTION

In recent years, the search for novel biomaterials with enhanced therapeutic properties has been a focus of research in biomedical science and material engineering over the past few years [1]. Among these, the development of multi-functional materials for antimicrobial and wound-healing applications has received much attention due to the growing prevalence of antibiotic resistance and the increasing demand for effective wound care solutions [2]. Synthesis and characterisation of β-CD conjugated carboxymethyl chitosan (CMCS) derivatives have been tried as a promising avenue to address these challenges where the properties from both components have been utilised synergistically [3]. Haemostasis, inflammation, proliferation and remodelling are all part of the complex physiological process wound healing. Materials that not only have antibacterial qualities but also encourage tissue regeneration and quicken the healing process are therefore desperately needed [4].

Chitosan is a natural polymer produced through the deacetylation of chitin and has been widely studied for its use in biomedicine owing to its intrinsic antibacterial activity, biocompatibility and biodegradability [5]. Common derivatives include carboxymethyl chitosan, N-succinyl chitosan, quaternised chitosan, phosphorylated chitosan and cyclodextrin conjugated chitosan [6]. In addition, chitosan has also been proven to be beneficial in wound healing by stimulating the proliferation of fibroblasts and the deposition of collagen [7]. However, due to the poor solubility of compound in water and physiological conditions has restricted its use. A water-soluble derivative of chitosan is carboxymethyl chitosan (CMCS), which is prepared through attaching carboxymethyl groups to

the backbone of chitosan. Such a mutation significantly increases its solubility over a large pH range, making it very versatile. Carboxymethyl chitosan (CMCS) also preserves key biological features of chitosan including antimicrobial activity and biocompatibility, while offering additional benefits such as enhanced hydrophilicity and greater potential for conjugation through various functionalization approaches [8]. Thus, CMCS is an ideal candidate for advanced biomaterial designs.

Cyclodextrins (CDs) are the cyclic oligosaccharides consisting of α-(1,4)-linked glucose units capable of forming host-guest inclusion complexes with a broad range of hydrophobic molecules. Among them, α-cyclodextrin (α-CD) is the most widely used owing to its moderate cavity size, biocompatibility and structural stability. However, the limited solubility and weak reactivity of native β-CD often restrict its direct use in aqueous biological systems. To overcome these challenges, numerous β-CD derivatives, such as carboxymethyl-β-CD, hydroxypropyl-β-CD and sulfobutyl ether-β-CD, have been synthesised to improve water solubility, functional group availability and molecular inclusion capacity [9,10]. Since its surface is hydrophilic while its core is hydrophobic, β-CD may interact with both polar and non-polar substances. The properties of β-CD make it an attractive component in drug delivery systems, antibacterial agents and wound dressings. β-CD and CMCS together produce a multifunctional material with improved performance [11,12]. Thus, the synergistic interaction improves the antimicrobial properties of this nanofibrous membrane and serves as a medium for wound healing through controlled drug delivery and tissue regeneration [13].

Parallel to this, carboxymethyl chitosan (CMCh), a water-soluble derivative of chitosan, has emerged as a promising biopolymer due to its biodegradability, non-toxicity and reactive amino and hydroxyl groups that allow further chemical conjugation. Earlier reports demonstrated that β-CD conjugation can significantly improve drug encapsulation efficiency, controlled release behaviour and antibacterial properties of chitosan-based materials [14-16]. These studies clearly demonstrate the potential of β-CD–modified chitosan systems but also reveal certain limitations, including limited control over the substitution pattern, poor structural stability and inconsistent biological performance.

The synthesis of β-CD conjugated CMCS derivatives involves techniques of chemical modification that ensure stability and functionality of the conjugate. Characterisation of the synthesised material is important in ensuring the success of the conjugation and evaluating its physico-chemical and biological properties [17]. Antimicrobial assays and *in vitro* wound-healing studies are conducted to determine its efficacy [18]. The β-CD conjugated CMCS derivative show a synergistic mechanism-based antimicrobial activity. Since CMCS is cationic in nature, it disrupts the cell membrane of the microbes; the inclusion properties of β-CD allow it to deliver the encapsulated antimicrobial agents precisely at the targeted site. This dual functionality is enormously beneficial in combating multi-drug resistant bacteria and biofilms because they pose highly significant impediments in wound management [19]. The reduction in microbial load helps create a more conducive environment for wound healing. Thus, keeping in mind about these facts, this study aims to synthesize and characterize β-cyclodextrin-conjugated carboxymethyl chitosan derivatives and evaluate their antimicrobial and wound-healing potential. The work further investigates their structural properties and biological performance to assess their suitability for biomedical applications.

EXPERIMENTAL

For this work, analytical grade methanol, ethanol and propan-2-ol were sourced from Thomas Baker, India, whereas NaOH, chloroacetic acid, DMF and benzaldehyde were purchased from Merck Life Science, India. β-Cyclodextrin were supplied by Sisco Research Laboratories of ≥ 98% purity. Squid pen were collected from the coastal areas of Bay of Bengal, India. Distilled water was used and filtration was accomplished using Whatman filter paper from. Without further purification, all chemicals were used as they were obtained.

Synthesis of β-CD conjugated carboxymethyl chitosan (CD-CMCh)

Isolation of chitosan from squid pen (*Dosidicus gigas*): Distilled water was used to clean the squid pen to remove surface contaminants. The pen was then treated with 1 M HCl solution to eliminate minerals. After thorough washing, it was demineralised by treatment with 3 M NaOH solution to obtain chitin. The deacetylation process was carried out by treating the demineralised squid pen with 50% NaOH solution for 24 h at 80 ºC, resulting in the removal of acetyl groups and the formation of chitosan.

Preparation of β-CD conjugated carboxymethyl chitosan (CD-CMCh): The sequential synthesis of β-CD conjugated carboxymethyl chitosan derivatives entailed many modifications to chitosan, resulting in intermediates labelled as complexes **1** to **4**.

Preparation of β-CS: The amino groups of chitosan were selectively protected by benzaldehyde so that the reaction could take place at the hydroxyl group on C-6. Here, 2.5 g of swollen chitosan in 30 mL of methanol was mixed with 10 mL of benzaldehyde in a step-by-step fashion. For a whole day, the mixture was left to stir at room temperature. Complex **1** (β-CS), the resulting solid, was filtered, washed extensively with methanol and then dried for 8 h at 60 ºC (**Scheme-I**).

Preparation of B-CMC: A 1.5 g of complex **2** were mixed with 1 mL of water-based NaOH solution (50 wt.%) at -4 ºC for 48 h to undergo alkalisation, then 1 g of chloroacetic acid in 10 mL of propan-2-ol was gradually added to the above solution. Overnight, at room temperature, the mixture was allowed to agitate. Complex **3** (B-CMC), obtained as a solid after filtration and washing with acetone and methanol, was subsequently dried at 60 ºC for 8 h (**Scheme-I**).

Preparation of CD-BCMCh: Then, 1 g of complex **3** was swollen in 80 mL of 0.1 M NaOH solution for 3 h, followed by filtration and drying. Subsequently, 1 g of β-CD dissolved in 20 mL of DMF was gradually added to the above mixture. The reaction was allowed to proceed under continuous stirring at room temperature for approximately 5 h. The resulting product, complex **3** (β-CD-B-CMC), was obtained as a solid after filtration and washing with acetone and methanol and was finally dried at 60 ºC for 8 h (**Scheme-I**).

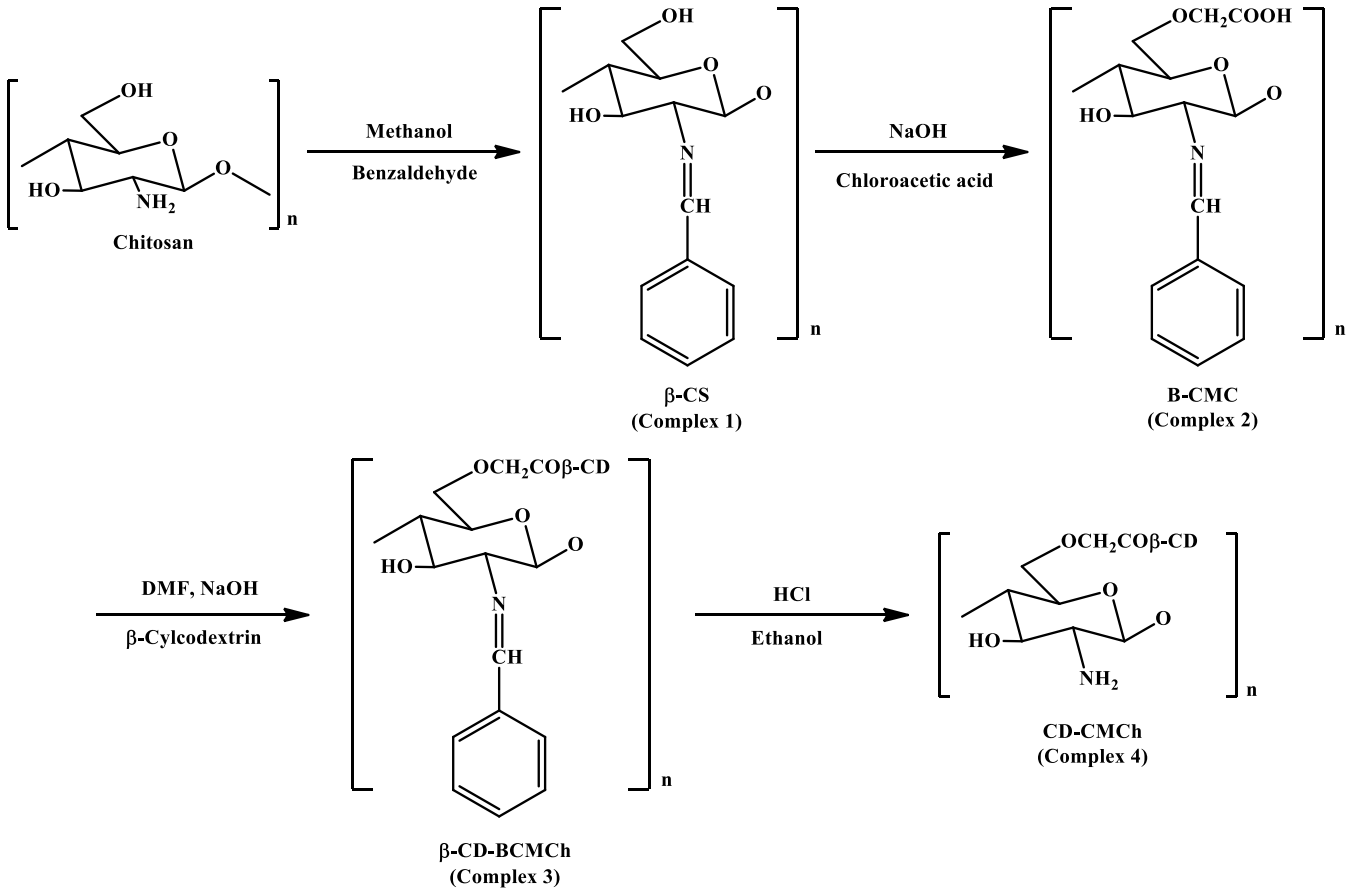

Scheme-I: Synthesis route of β-cyclodextrin conjugated carboxymethyl chitosan (complex **4**)

Preparation of CD-CMCh: The final product was prepared by reacting 2 g of complex **3** with 60 mL of an ethanolic solution that contained 0.24 mol/L of HCl. At room temperature, the ingredients were stirred for a whole day. Filtering, cleaning and drying were carried out to obtain complex **4**, the solid product. The β-CD conjugated carboxymethyl chitosan can be obtained by drying the product in a vacuum oven at 55 ºC for 8 h with required yield (**Scheme-I**).

Characterisation: To evaluate the synthesised β-cyclodextrin conjugated carboxymethyl chitosan derivative, several characterisation techniques were employed: The FTIR spectra were recorded using an attenuated total reflection (ATR) mode on a Nicolet iS-50 from Thermo-Scientific. An XtaLAB Synergy Dualflex Pilatus 300K diffractometer was used for X-ray diffraction (XRD) examination in order to assess the crystallinity of the conjugated derivative. ^{1}H NMR and ^{13}C NMR spectra of 2F and *i*-CTs were recorded using BRUKER NMR spectrometer-400 MHz with DMSO as solvent at 298.5 K. Surface morphology and shape of nanosponges obtained from the conjugated derivative were studied using a JSM5910 scanning electron microscope. Samples were mounted on metal stubs, coated with a 300 Å gold layer *via* sputtering and analysed at different magnifications to study size, texture and structural integrity. The 'energy dispersive X-ray spectroscopy (EDS) spectrum' for the synthesised β-cyclodextrin conjugated carboxymethyl chitosan derivative would reveal the elemental composition of the material.

Biological studies: The antimicrobial activity was tested against specific bacterial and fungal strain. The bacterial strains *viz. Staphylococcus aureus*, *Escherichia coli* and *Klebsiella pnemoniae*, representing Gram-negative and Gram-positive bacteria, respectively. For fungal activity, strains *viz. Candida albicans*, *Aspergillus niger*, *Trichoderma viride* were employed. These standard strains are commonly used as model organisms to assess the efficacy of antimicrobial agents. A wound healing assay was conducted to assess cell migration. The Vero cell line was seeded into a six-well plate and cultured for 24 h to allow cell attachment and growth. Upon reaching sufficient confluence, a scratch was created, and the experiment was initiated. Subsequently, 1 mL of the sample at a concentration of 100 μg/mL was added to each well, followed by incubation. After 24 h, the cells were examined to evaluate migration and wound closure.

Statistical analysis: The disc diffusion results were statistically analysed using one-way ANOVA followed by Tukey's HSD multiple comparisons of means using R (version 3.5.1) [20]. Data are presented as boxplots. Differences were considered significant for $p < 0.05$. Values were reported as means ± standard deviations and statistical means were compared by *t*-test with $p < 0.05$.

RESULTS AND DISCUSSION

FT-IR spectral studies: IR spectra of all the compounds (Fig. 1) shows broad band around 3600-3200 cm^{-1} due to the

stretching vibration of –OH. The broad absorption band observed in the range of 2900-2800 cm^{-1} is attributed to –NH vibrations and intermolecular hydrogen bonding within the polysaccharide structure, while the peak around 2900 cm^{-1} corresponds to the symmetric stretching vibrations of –CH and $–CH_2$ groups in the pyranose ring. The characteristic peaks at 1023-1019 cm^{-1} confirm the saccharide framework. The absorption bands at 1648, 1638, 1602, 1637 and 1569 cm^{-1} in derivatives **1-4** confirmed the successful deacetylation of chitosan. In native chitosan, a doublet at 3359 and 3190 cm^{-1} is observed; however, this feature disappears in derivative **1** and is replaced by a single peak at 3411 cm^{-1}, suggesting bond formation between the –NH group and benzaldehyde at the C2 position. The peaks at 683 and 748 cm^{-1} are associated with substituted benzene rings, while bands in the range of 1590-1490 cm^{-1} correspond to aromatic C=C and C=N stretching vibrations. A strong absorption near 1560 cm^{-1} is assigned to the asymmetric stretching of COO^- groups, indicating the substitution of carboxy-methyl groups at the C6 position. Furthermore, peaks at 1590 and 900 cm^{-1} are attributed to C=O vibrations and the α-pyranose ring of β-cyclodextrin, respectively. In derivative **4**, the disappearance of peaks at 1492, 1471, 1369, 699 and 753 cm^{-1} confirms the removal of benzaldehyde moieties.

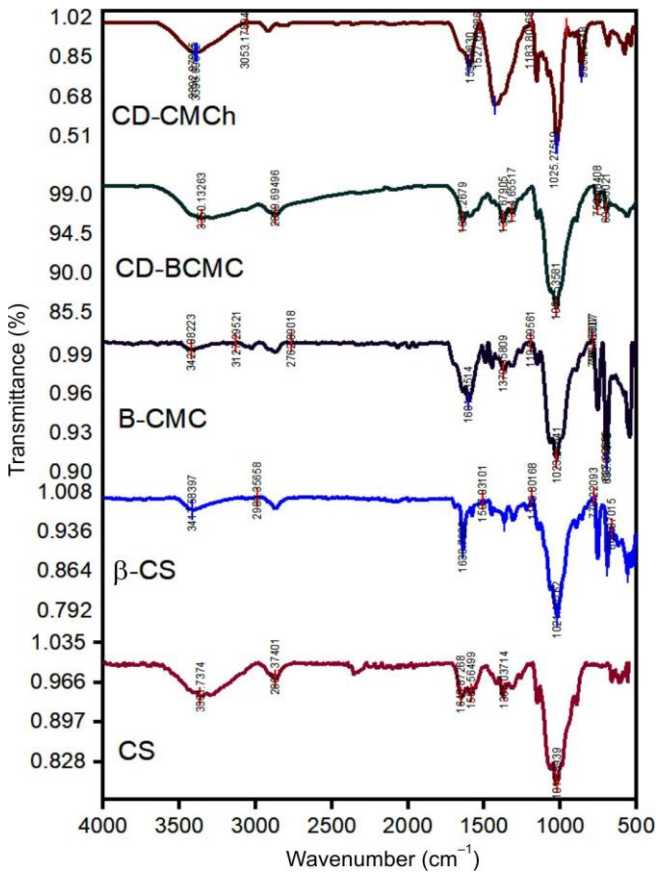

Fig. 1. FT-IR spectra of the chitosan and its derivatives

XRD studies: The XRD pattern of CD-CMCh (complex **4**) indicates a predominantly crystalline structure, comprising approximately 91.1% crystalline and 8.9% amorphous content (Fig. 2). The broad diffraction feature observed in the 2θ range

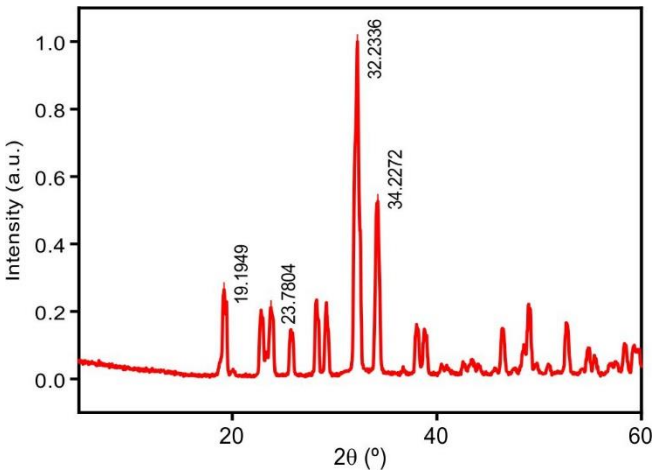

Fig. 2. XRD spectrum of CD-CMCh (complex **4**)

of 20-30º suggests the presence of an amorphous phase, which is the characteristic of partially disordered polysaccharide systems. The distinct and sharp diffraction peaks at higher 2θ values confirm the formation of a well-defined crystalline phase. The peak at 2θ ≈ 22.8º corresponds to the characteristic reflection of native chitosan, while the diffraction peak at 2θ ≈ 35.73º can be attributed to contributions from carboxymethyl chitosan (CMC) and β-CD [21]. The appearance of a crystalline peak at 2θ ≈ 19.18º is indicative of the presence of β-CD within the composite structure [22,23].

^{1}H NMR and ^{13}C NMR spectra: The ^{1}H NMR spectral analysis of β-CD-CMCh signifies the attachment of β-CD to CMC. The chitosan's anomeric (H_1) proton clearly exhibits the largest shift from 4.705 ppm in CMCh to δ 4.971 ppm in CD-CMCh, which suggests an interaction between the two parts. Furthermore, the new peaks from δ 3.0-4.0 ppm region in the CD-CMCh spectrum confirms the presence of chitosan and the glucose protons of β-CD, thus confirming the incorporation. In addition, the peaks for CMCh that exhibited two overlapping peaks at δ 2.62-2.95 ppm to broad peak centered in δ 2.62-2.95 ppm in CD-CMCh suggest an increase in the electronic environment as a result of conjugation. There are also changes in the range δ 7.38-7.77 ppm, which was supposed to be present on CMCh but are not or have been greatly reduced. This suggests that some structural changes have taken place, probably due to the formation of a stable complex. The observed shifts in spectral positions provide strong evidence for the successful synthesis of the CD-CMCh conjugate. The β-CD and CMCh moieties exhibit characteristic signals in the ^{13}C NMR spectrum of the CD-CMCh conjugate. The glucose ring carbons (C2–C5) resonate between 72-85 ppm, while the anomeric carbon (C_1) of β-CD and chitosan resonates within 101-105 ppm, being normally found between 60 and 65 ppm. Furthermore, the presence of carboxymethyl groups is confirmed by the characteristic signals in the ^{13}C NMR spectrum, for example, the carboxyl ($–COO^-$) carbon appears at 175-180 ppm, $O-CH_2–COO^-$ resonates in the 68-75 ppm region, and $N-CH_2–COO^-$ is observed at 45-50 ppm. The peaks at ~ 178 and 101 ppm are attributed to the carboxyl and anomeric carbons, respectively, while the signals corresponding to the glucose ring carbons are detected in the 60-81 ppm range.

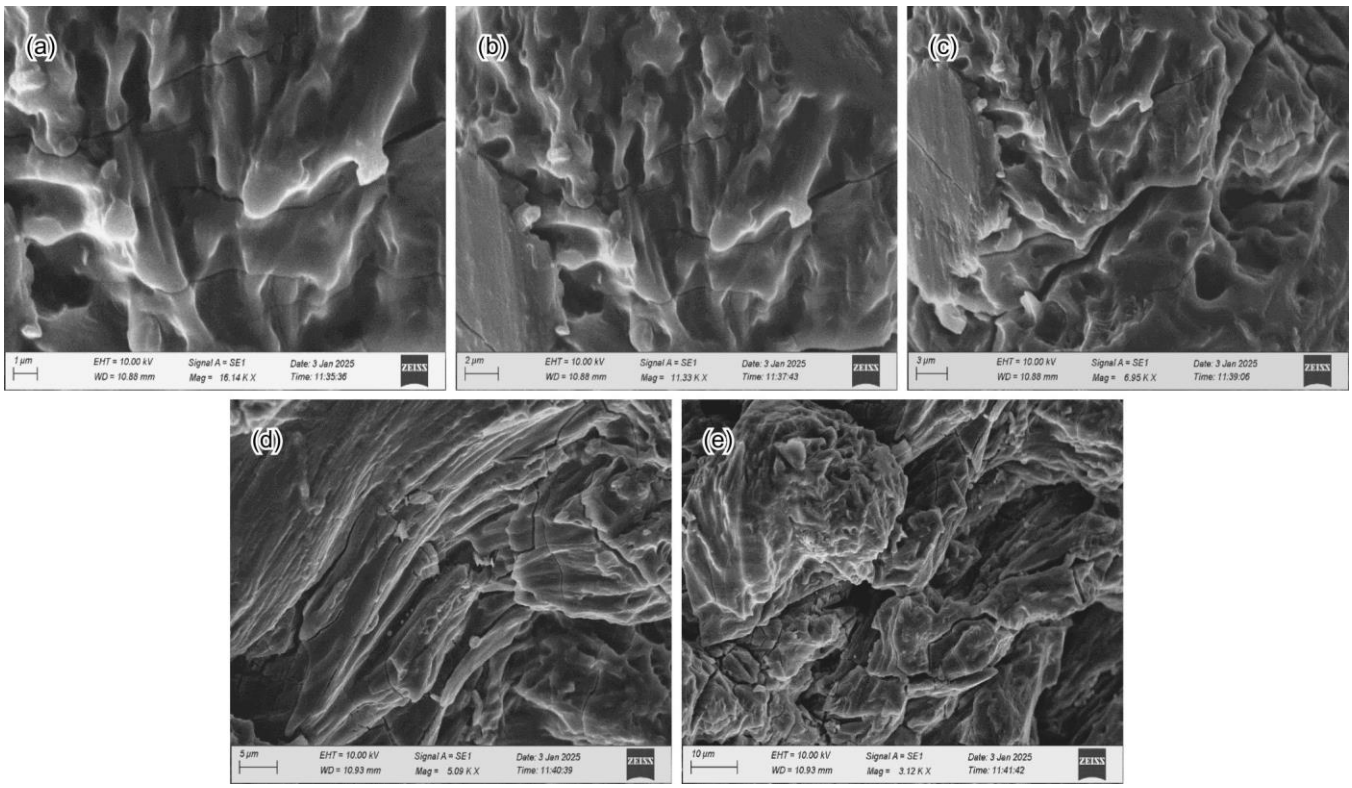

Fig. 3. SEM images of CD-CMCh (complex **4**)

These spectral features collectively support the successful formation of the CD-CMCh conjugate.

SEM studies: The SEM images (Fig. 3) of CD-CMCh (complex **4**) at different magnifications provide insight into the surface architecture of the synthesized material. The micrographs reveal uneven and non-uniform surface features, suggesting noticeable structural changes. Regions appearing brighter are associated with stronger electron scattering, which can be linked to variations in surface texture, composition or crystalline arrangement. Conversely, darker areas indicate relatively smoother and less dense regions. Upon closer examination, the images show folded, layered and porous morphologies typical of the polymeric based composites [24,25], which enhance the effective surface area and improve interactions with surrounding environments, which is advantageous for potential biomedical applications.

EDS studies: The EDS spectrum illustrates the elemental composition of a CD-CMCh (complex **4**) material. The spectral peaks represent different elements found in the sample. The height of each peak is directly proportional to the concentration of the corresponding element. The most significant peak in this spectrum is designated "O", signifying the presence of oxygen with 54%. Additional components identified are carbon (30%) and nitrogen (14%) (Fig. 4). The spectrum furthermore displays minor peaks, maybe attributable to trace quantities of other elements [26,27].

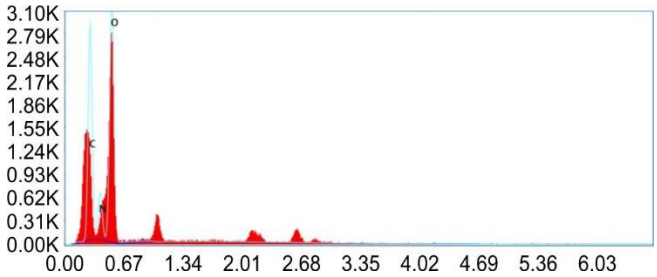

Fig. 4. EDS spectrum of CD-CMCh (complex **4**)

Biological studies

Antibacterial activity: The antibacterial activity of the CD-CMCh (complex **4**) material was evaluated against *S. aureus*, *E. coli* and *K. pneumoniae* at concentrations of 1000, 750 and 500 μg/mL. The results demonstrate a clear concentration dependent inhibitory effect on microbial growth (Table-1). Among the tested strains, *S. aureus* exhibited the highest susceptibility, with zones of inhibition measuring 13 ± 2 mm, 10.7 ± 1.2 mm and 9.7 ± 0.6 mm at 1000, 750 and 500 μg/mL, respectively. In comparison, *E. coli* showed relatively lower sensitivity, with inhibition zones ranging from 8 to 9 mm across the tested concentrations, whereas *K. pneumoniae* displayed moderate susceptibility, with inhibition zones of 11 ± 2 mm, 8.3 ± 0.6 mm and 7 ± 1 mm.

The antibacterial effect of complex **4** was compared with the standard antibiotic ampicillin (20 μL/disc), which exhibited higher activity against *S. aureus* and comparable effects against *K. pneumoniae*. Statistical analysis confirmed that the observed differences were significant ($p < 0.05$). These findings indicate that the material possesses notable antibacterial properties, particularly against Gram-positive bacteria, with effectiveness influenced by concentration [28]. Based on the other reported similar chitosan derivatives, it is found that CD-CMCh significant antibacterial activity (Table-2), with

TABLE-1
ANTIBACTERIAL ACTIVITY DATA OF CD-CMCh (COMPLEX **4**) AT DIFFERENT CONCENTRATIONS

Organisms	Zone of inhibition (mm)			
	1000 μg/mL	750 μg/mL	500 μg/mL	Ampicillin (20 μL/disc)
Staphylococcus aureus	13 ± 2	10.7 ± 1.2	9.7 ± 0.6	21.7 ± 0.6
Escherichia coli	9 ± 1	8 ± 0	8 ± 1	10.3 ± 0.6
Klebsiella pnemoniae	11 ± 2	8.3 ± 0.6	7 ± 1	11.7 ± 0.6

± Standard deviation (n = 3). Values in the same column are significantly different at (*$p < 0.05$) based on Duncan's multiple range test.

TABLE-2
COMPARATIVE ANTIBACTERIAL ACTIVITY DATA OF THE SYNTHESIZED CD-CMCh (COMPLEX **4**) ALONG WITH THE SIMILAR REPORTED SYSTEMS

Compound	Organisms	Bacterial activity (mm)	Ref.
β-CD-MAH-VBDMH	*Staphylococcus aureus* and *Escherichia coli*	10 and 13	[20]
O-CMC	*Staphylococcus aureus* and *Escherichia coli*	1 and 10	[29]
O-CMC–PEG	*Staphylococcus aureus* and *Escherichia coli*	17.5 ± 0.3 and 13.2 ± 0.4	[30]
LEO/HPCD	*Staphylococcus aureus* and *Escherichia coli*	15.47 ± 0.5 and 13.67 ± 0.3	[31]
CD-CMCh	*Staphylococcus aureus*, *Escherichia coli* and *Klebsiella pneumoniae* at 1000 μg/mL	13 ± 2, 9 ± 1 and 11 ± 2.0	Present study

higher effectiveness against *S. aureus* compared to Gram-negative strains indicating that β-cyclodextrin incorporation enhances antimicrobial properties.

Antifungal activity: The antifungal performance of the CD-CMCh (complex **4**) was assessed using the agar diffusion method against *A. niger*, *T. viride* and *C. albicans* at concentrations of 1000, 750 and 500 μg/mL (Table-3). The results indicate that fungal growth inhibition increased with concentration for all tested strains. *A. niger* showed the highest sensitivity, with a maximum inhibition zone of 19 ± 5.7 mm, while *T. viride* and *C. albicans* exhibited moderate inhibition across the tested concentrations. Amphotericin B (20 μL/disc) exhibited higher inhibition zones for all strains and statistical analysis confirmed significant differences ($p < 0.05$). These findings indicate that antifungal activity depends on both concentration and fungal species. Moreover, CD-CMCh exhibited also significant antifungal activity, particularly against *A. niger*, with comparatively moderate effects on *T. viride* and *C. albicans* (Table-4), indicating effective functionalization.

Wound healing activity: The wound healing experiment utilizing the Vero cell line exhibited increased cell migration and proliferation. Following 24 h of incubation with the synthesised derivative at 100 μg/mL, a significant decrease in the wound gap was detected microscopically. It shows that CD-CMCh (complex **4**) capability to expedite wound healing and tissue regeneration (Fig. 5). This indicates the ability of complex **4** to promote cell migration and accelerate wound closure effectively within a short period.

Conclusion

This work reports the successful development of a β-cyclodextrin-linked carboxymethyl chitosan (CD-CMCh) material, with its structure and properties characterized. The results indicate that the modification led to improved structural organisation along with a porous and irregular surface, features that are beneficial for biological interactions. The material demonstrated meaningful antibacterial and antifungal performance, particularly against *S. aureus* and *A. niger*, with activity influenced by concentration. In addition, the wound healing study showed enhanced cell migration and faster closure of the wound area, suggesting its ability to support tissue repair processes. The incorporation of β-cyclodextrin into the chitosan framework improves both functional and biological characteristics.

TABLE-3
ANTIFUNGAL ACTIVITY DATA OF CD-CMCh (COMPLEX **4**) AT DIFFERENT CONCENTRATIONS

Organisms	Zone of inhibition (mm)			
	1000 μg/mL	750 μg/mL	500 μg/mL	Amphotericin B (20 μL/disc)
Aspergillus niger	19 ± 5.7	15 ± 6.0	16.37 ± 7.6	32 ± 1.0
Trichoderma viride	13.3 ± 3.5	10.7 ± 4.5	12.7 ± 5.0	26.7 ± 1.2
Candida albicans	12 ± 4.0	14 ± 5.6	14.3 ± 2.1	41 ± 1.0

± Standard deviation (n = 3). Values in the same column are significantly different at (*$p < 0.05$) based on Duncan's multiple range test.

TABLE-4
COMPARATIVE ANTIFUNGAL ACTIVITY DATA OF THE SYNTHESIZED CD-CMCh (COMPLEX **4**) ALONG WITH THE SIMILAR REPORTED SYSTEMS

Compound	Organisms	Fungal activity (mm)	Ref.
LEO/HPCD	*Candida albicans*	17.73 ± 0.4	[31]
β-CD–EO	*Candida albicans*	No effect as compound shows activity on coated with tablet	[32]
CD-CMCh	*Aspergillus niger*, *Trichoderma viride* and *Candida albicans* at 1000 μg/mL	19 ± 5.7, 13.3 ± 3.5 and 12 ± 4	Present study

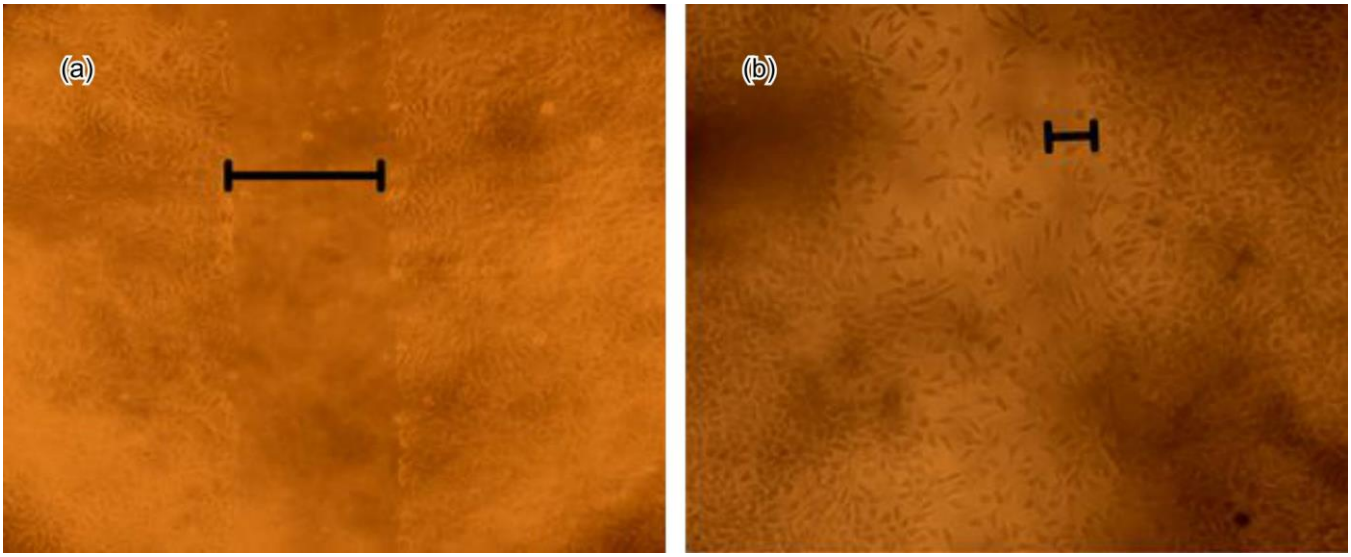

Fig. 5. Wound healing assay in Vero cells after 24 h incubation with CD-CMCh (complex **4**) at 100 µg/mL. (a) Control showing wider wound gap and (b) treated cells showing significant gap closure, indicating enhanced cell migration and tissue regeneration.

ACKNOWLEDGEMENTS

The authors gratefully thank Dr. I Seethalakshmi, Life Teck Research centre for their support towards biomedical evaluation, Saveetha Dental college, IIT-Chennai, Crecent University for providing the characterisation facilities.

CONFLICT OF INTEREST

The authors declare that there is no conflict of interests regarding the publication of this article.

DECLARATION OF AI-ASSISTED TECHNOLOGIES

During the preparation of this manuscript, the authors used an AI-assisted tool(s) to improve the language. The authors reviewed and edited the content and take full responsibility for the published work.

REFERENCES

1. B. Tian, S. Hua and J. Liu, *Carbohydr. Polym.*, **315**, 120972 (2023); https://doi.org/10.1016/j.carbpol.2023.120972
2. W. Chen, H. Cheng, L. Chen, X. Zhan and W. Xia, *Carbohydr. Polym.*, **284**, 119185 (2022); https://doi.org/10.1016/j.carbpol.2022.119185
3. C. Carrera, C. Bengoechea, F. Carrillo and N. Calero, *Food Hydrocoll.*, **137**, 108383 (2023); https://doi.org/10.1016/j.foodhyd.2022.108383
4. W. Wang, C. Xue and X. Mao, *Int. J. Biol. Macromol.*, **164**, 4532 (2020); https://doi.org/10.1016/j.ijbiomac.2020.09.042
5. X. Tong, W. Pan, T. Su, M. Zhang, W. Dong and X. Qi, *React. Funct. Polym.*, **148**, 104501 (2020); https://doi.org/10.1016/j.reactfunctpolym.2020.104501
6. A. El-Araby, W. Janati, R. Ullah, S. Ercisli and F. Errachidi, *Front Chem.*, **11**, 1327426 (2024); https://doi.org/10.3389/fchem.2023.1327426
7. E. Mohammadi, H. Daraei, R. Ghanbari, S.D. Athar, Y. Zandsalimi, A. Ziaee, A. Maleki and K. Yetilmezsoy, *J. Mol. Liq.*, **273**, 116 (2019); https://doi.org/10.1016/j.molliq.2018.10.019
8. L. Wei, J. Zhang, W. Tan, G. Wang, Q. Li, F. Dong and Z. Guo, *Int. J. Biol. Macromol.*, **179**, 292 (2021); https://doi.org/10.1016/j.ijbiomac.2021.02.184
9. T. Loftsson and D. Duchene, *Int. J. Pharm.*, **329**, 1 (2007); https://doi.org/10.1016/j.ijpharm.2006.10.044
10. T. Loftsson, M.D. Moya-Ortega, C. Alvarez-Lorenzo and A. Concheiro, *J. Pharm. Pharmacol.*, **68**, 544 (2016); https://doi.org/10.1111/jphp.12427
11. A.A. Hamed, I.A. Abdelhamid, G.R. Saad, N.A. Elkady and M.Z. Elsabee, *Int. J. Biol. Macromol.*, **153**, 492 (2020); https://doi.org/10.1016/j.ijbiomac.2020.02.302
12. J. Sun, J. Chen, Y. Bi, Y. Xiao, L. Ding and W. Bai, *Food Chem.*, **370**, 130933 (2022); https://doi.org/10.1016/j.foodchem.2021.130933
13. N.A. Negm, H.H. Hefni, A.A. Abd-Elaal, E.A. Badr and M.T. Abou Kana, *Int. J. Biol. Macromol.*, **152**, 681 (2020); https://doi.org/10.1016/j.ijbiomac.2020.02.196
14. T.S. Anirudhan, P.L. Divya and J. Nima, *Chem. Eng. J.*, **284**, 1259 (2016); https://doi.org/10.1016/j.cej.2015.09.057
15. J. Ji, S. Hao, W. Liu, J. Zhang, D. Wu and Y. Xu, *Polym. Bull.*, **67**, 1201 (2011); https://doi.org/10.1007/s00289-011-0449-4
16. M. Song, L. Li, Y. Zhang, K. Chen, H. Wang and R. Gong, *React. Funct. Polym.*, **117**, 10 (2017); https://doi.org/10.1016/j.reactfunctpolym.2017.05.008
17. J. Wang and S. Zhuang, *J. Clean. Prod.*, **355**, 131825 (2022); https://doi.org/10.1016/j.jclepro.2022.131825
18. A. Madni, R. Kousar, N. Naeem and F. Wahid, *J. Biores. Bioproducts*, **6**, 11 (2021); https://doi.org/10.21967/jbb.v4i1.189
19. W.-Y. Ding, S.-D. Zheng, Y. Qin, F. Yu, J.-W. Bai, W.-Q. Cui, T. Yu, X.-R. Chen, G. Bello-Onaghise and Y.-H. Li, *Front. Chem.*, **6**, 657 (2019); https://doi.org/10.3389/fchem.2018.00657
20. L. Sun, Y. Du, L. Fan, X. Chen and J. Yang, *Polymer*, **47**, 1796 (2006); https://doi.org/10.1016/j.polymer.2006.01.073
21. A. Nabili, A. Fattoum, R. Passas and E. Elalout, *Cellulose Chem. Technol*, **50**, 1015 (2016).
22. M. Prabaharan and S. Gong, *Carbohydr. Polym.*, **73**, 117 (2008); https://doi.org/10.1016/j.carbpol.2007.11.005
23. M. Shakir, R. Jolly, M.S. Khan, A. Rauf and S. Kazmi, *Int. J. Biol. Macromol.*, **93**, 276 (2016); https://doi.org/10.1016/j.ijbiomac.2016.08.046
24. A. Ravaglioli, A. Krajewski, G.C. Celotti, A. Piancastelli, B. Bacchini, L. Montanari, G. Zama and L. Piombi, *Biomaterials*, **17**, 617 (1996); https://doi.org/10.1016/0142-9612(96)88712-6

25. M.A. Ali, K.A. Aswathy, G. Munuswamy-Ramanujam and V. Jaisankar, *Int. J. Biol. Macromol.*, **225**, 1575 (2023); https://doi.org/10.1016/j.ijbiomac.2022.11.214
26. C. Rey, A. Hina, A. Tofighi and M.J. Glimcher, *Cells Mater.*, **5**, 345 (1995).
27. Y. Chen, J. Yan, Y. Zhang, W. Chen, Z. Wang and L. Wang, *J. Polym. Environ.*, **30**, 1012 (2022); https://doi.org/10.1007/s10924-021-02255-7
28. Z. Shariatinia, *Int. J. Biol. Macromol.*, **120**, 1406 (2018); https://doi.org/10.1016/j.ijbiomac.2018.09.131
29. B. Yang, B. Liu, Y. Gao, J. Wei, G. Li, H. Zhang, L. Wang and Z. Hou, *Sci. Rep.*, **14**, 10825 (2024); https://doi.org/10.1038/s41598-024-61642-x
30. R. Li, J. Dou, Q. Jiang, J. Li, Z. Xie, J. Liang and X. Ren, *Chem. Eng. J.*, **248**, 264 (2014); https://doi.org/10.1016/j.cej.2014.03.042
31. C. Yuan, Y. Wang, Y. Liu and B. Cui, *Ind. Crops Prod.*, **130**, 104 (2019); https://doi.org/10.1016/j.indcrop.2018.12.067
32. A. Arrais, M. Manzoni, A. Cattaneo, V. Gianotti, N. Massa, G. Novello, A. Caramaschi, E. Gamalero and E. Bona, *Appl. Sci.*, **11**, 6597 (2021); https://doi.org/10.3390/app11146597